Planar, Fast, Reliable, Single-Heterojunction Light-Emitting Diodes for Optical Links

By V. G. KERAMIDAS, G. W. BERKSTRESSER, and C. L. ZIPFEL

(Manuscript received April 29, 1980)

The properties, fabrication and performance of planar (i.e., without an etched well), single heterojunction $Ga_{1-x}Al_xAs:Te—GaAs:Ge$ fast LEDs, developed for use in optical data links, are discussed in this paper. The LEDs consist totally of epitaxially grown material. Current confinement achieved by contact area restriction increases current density and localizes electroluminescence for efficient coupling into a fiber. The peak wavelength of emission is at ≈ 900 nm with a full width at half-maximum of ≈ 50 nm. Electroluminescent rise and fall times are ≈ 3 ns each with pre-bias, making these LEDs adequate for data transmission rates as high as 100 Mb/s. At 700 A/cm^2, the LEDs launch 100 μW of optical power into a 0.36 numerical aperture (NA) and 125-μm core-diameter, step-index fiber or 10 μW into a 0.23-NA, 55-μm core-diameter, graded-index fiber. The LEDs are highly reliable with extrapolated mean time to failure of 2.7×10^7 hours at junction current density of 700 A/cm^2 and junction temperature of 74°C. These LEDs have been used as sources in prototype subsystems under development for use in electronic switching systems.

I. INTRODUCTION

In a recent publication[1] we reported on a broad-area (junction area extending over the full area of the chip), low-current-density, simple-geometry LED with exceptional reliability. These broad-area LEDs, at 67 A/cm^2 current density, launched 30 μW of butt-coupled optical power into a fiber with 0.36 numerical aperture (NA) and a 125-μm

core diameter[2] and were used as sources in prototype optical-link electronic switching systems with low optical power requirements.[3]

In this paper, we report on planar LEDs, i.e., devices which consist totally of material grown by liquid phase epitaxy (LPE). This device structure eliminates the need for the etched well, characteristic of Burrus-type devices,[4] resulting in over 90-percent device fabrication yield. Uniform material of 7.0 cm^2 can be grown on a substrate during a single crystal growth run yielding ~1500 LEDs. These LEDs launch 100 μW of butt-coupled optical power into a 0.36-NA, 125-μm core-diameter fiber and 10 μW into a fiber with 0.23 NA and 55-μm core diameter. The improvements over the broad area device result from current crowding by contact area restriction (from full area to 50-μm diameter dot) to increase the current density (from 67 A/cm^2 to 700 A/cm^2) for increased brightness. Furthermore, the localized emission region couples the light more efficiently into the fiber. This simple LED structure, which can be grown on large areas and fabricated with high yield, is exceptionally reliable with predicted failure rates of 1 FIT for a 40-year service life.

Large numbers of these devices have been used for the development of the LED-optical-fiber packaging technology and in prototype subsystems currently under development for optical links used in electronic switching systems.

II. LED STRUCTURE AND FABRICATION

The LED structure reported in this paper is a planar, single heterojunction. It consists totally of epitaxially grown material: a graded bandgap n$-$Ga$_{1-x}$Al$_x$As:Te "window" layer, transparent to the emitted radiation, and a p-GaAs:Ge active layer. Growing the window layer sufficiently thick (30–50 μm) eliminated the need for retaining part of the GaAs substrate. The removal of the substrate, which is opaque to the emitted radiation, eliminated the need for an etched well, characteristic of Burrus-type structures,[4] resulting in a planar LED structure shown in Fig. 1. The GaAs substrate was selectively removed from the epitaxial layers by a preferential chemical etch in a two-step process. A preliminary etch solution, consisting of equal parts by volume of 30-percent H$_2$O$_2$ and NH$_4$OH (pH = 9.6), was used for the removal of most of the substrate. A "stop etch" solution,[5] consisting of 100 parts by volume of 30-percent H$_2$O$_2$ and ~4 parts of NH$_4$OH, adjusted to a pH of 8.5 ± 0.2 at T = 23 ± 1°C, was used to complete the removal.

Ohmic contacts were made by evaporating 35 Å Al, 500 Å Sn, and 30,000 Å Au on the n-side and 800 Å of 1 weight-percent Be in Au and 2,100 Å of Au on the p-side with subsequent alloying.[6] The n-type contact consists of a solid field of metallization except for a circular window 112 μm in radius (see Fig. 1) where the fiber is ultimately

placed close to the LED surface. This n-contact configuration optimizes current spreading from the metallized region towards the center of the device. The 50-μm diameter dot p-type contact is centered under the circular opening of the n-contact (see Fig. 1). Device fabrication is completed by dicing the material into 600×600-μm square dice. The chips are etched in HNO_3 to remove saw damage and are finally mounted p-side down onto a TO-18, or power header. Planar LEDs can be fabricated with over 90-percent device fabrication yields, much higher than the best yields attainable in Burrus-type devices.

By reducing the contact dimension to a 50-μm diameter dot aligned under the fiber and adjusting the p-layer thickness and resistivity, an increase in the effective current density is achieved that results in higher surface brightness. Such techniques have been used previously for optical communications LED fabrication.[7, 8] Another approach to current confinement is the restriction of the junction area. This can be attained by preferential chemical etching, or proton implantation.[9-12]

III. CRYSTAL GROWTH AND MATERIALS CONSIDERATIONS

The materials for the planar LED structure discussed here are grown by liquid phase epitaxy (LPE) on [100] oriented, chemically polished GaAs substrates. The fixture used for growth is a sliding boat system. The boat resides in a quartz tube that is continuously purged with Pd purified H_2. The growth procedure is similar to that described elsewhere[1] with the added step of interrupting the growth by pushing the substrate away from the second melt when the desired thickness is achieved. The melts used have the following composition: Melt I has an approximate atom fraction composition of $X_{Ga} = 0.928$, $X_{As} = 0.070$, $X_{Al} = 0.00253$, and $X_{Te} = 0.0000455$. Melt II has an approximate atom fraction composition of $X_{Ga} = 0.898$, $X_{As} = 0.067$, $X_{Ge} = 0.0333$. To avoid backmelting, the amount of GaAs source material added to
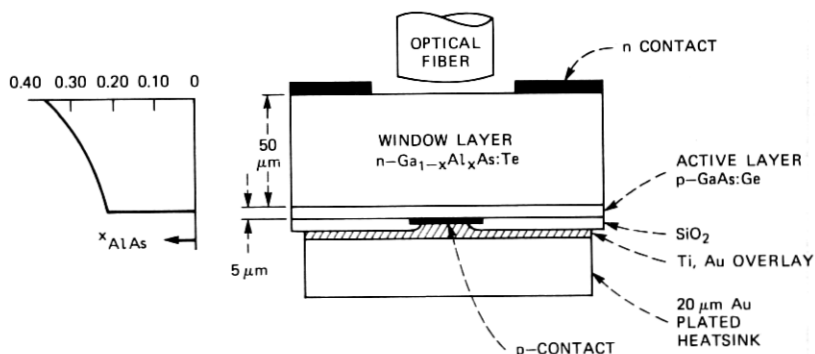

Fig. 1—Planar, single heterojunction, optical-link LED structure and compositional profile.

solution II was chosen so that this solution is near equilibrium at the temperature when the substrate and epitaxial layer come into contact with it. The exact melt compositional control makes it possible to grow on 7.3 cm^2 substrates in a single run with minor edge growth and 100-percent wipe off. After trimming the edge growth, ~7.0 cm^2 of the material can be used yielding ~1500 LEDs.

The physical properties and dimensions of the heterojunction layers are important to the device performance and fabrication. The graded bandgap n-type $Ga_{1-x}Al_x As$ layer serves two functions: (i) it controls the carrier injection and (ii) it provides a low-loss radiation window for photons traveling towards the fiber. Under forward bias, the wider bandgap n-$Ga_{1-x}Al_x As$ presents a potential barrier for holes. Thus, even at higher injection levels, only electrons are injected into the heavily doped p-type GaAs region where they recombine to produce photons with energy near that of the GaAs bandgap ≈1.4 eV or 900 nm. Photons emitted into the wider bandgap $Ga_{1-x}Al_x As$ layer travel towards the fiber through a radiation window. Photons emitted into the GaAs region are absorbed. Limitations on the n-layer thickness were for the following reasons. The initial value of x in the $Ga_{1-x}Al_x As$ is ≈0.35. Under the growth conditions used, Al, due to its high distribution coefficient, segregates strongly in favor of the solid. As growth proceeds, Al is depleted from the melt and x decreases. For thick n-layers, x at the p-n junction could decrease enough to increase absorption losses and/or reduce carrier injection into the p-layer. If a too thin n-layer is grown, the epitaxial material would be too fragile to be handled during device fabrication.

The active p-type GaAs layer is heavily doped with Ge to ~2 × 10^{19} cm^3 and is 5 μm thick. This carrier density value is the upper limit in doping before the electroluminescence efficiency[1] and the butt-coupled power into the fiber begin to decrease. The experimentally determined optimum p-layer thickness of 5 μm is approximately equal to the minority carrier diffusion length measured on ~10^{19} cm^{-3} p-type GaAs using electron beam-induced current (EBIC)[13] and as reported elsewhere.[14] As discussed in Ref. 13, the product of the calculated external quantum efficiency η_{SH} and the current density J for a single heterojunction $Ga_{1-x}Al_x As$—GaAs LED also peaks at a p-layer thickness of ~3 to 4 μm. $\eta_{SH} \times J$ is limited by surface recombination for thin layers and self-absorption or current spreading for thick layers. The use of a 5-μm p-layer also permits the achievement of reproducible uniform layer thickness over the ~7 cm^2 area of epitaxially grown material.

IV. LED PERFORMANCE

The external quantum efficiency of these LEDs shows a relatively small change over a wide range of applied current (0.1 to 100 mA).

The spectral emission peaks at ≈900 nm, with a full width at half maximum of ≈50 nm.

The electroluminescent rise (τ_R) and fall (τ_F) times of the LED spectral output (10 to 90 percent), for the typical carrier concentrations of $n \approx 7 \times 10^{17}$ cm^{-3} and $p \approx 2 \times 10^{19}$ cm^{-3}, are 5 and 6 ns, respectively, when measured without pre-bias. The junction capacitance at zero bias is ≈130 pF. With the use of a TTL LED driver, a built-in prebias of 1.2 V reduces the charging time for the LED depletion layer capacitance. By adding current spikes to the leading and trailing edges of the LED current pulse, the LED is rapidly charged and discharged of injected minority carriers. As a result, τ_R and τ_F are speeded up to 3 ns each. These rise and fall times are now fast enough for 100 Mb/s nonreturn to zero (NRZ) operation with negligible pulse jitter and asymmetry.

Finally, at an external drive current of 60 mA of optical power, 100 μW has been coupled into a step-index fiber with an NA = 0.36 and core diameter = 125 μm, and 10 μW into a graded-index fiber with NA = 0.23 and core diameter = 55 μm. Typical values of power coupled into both the above fibers as a function of the external drive current are shown in Figs. 2 and 3, respectively. To assess the butt-coupled power difference of a planar LED structure where the fiber is ~50 μm away from the photon-emitting plane and a Burrus-type LED where the fiber is ~2 μm from the junction, planar LEDs were converted to etched well LEDs by removing all but ~2 μm of the window layer. The thick window layer of the planar LED described here reduces the butt-
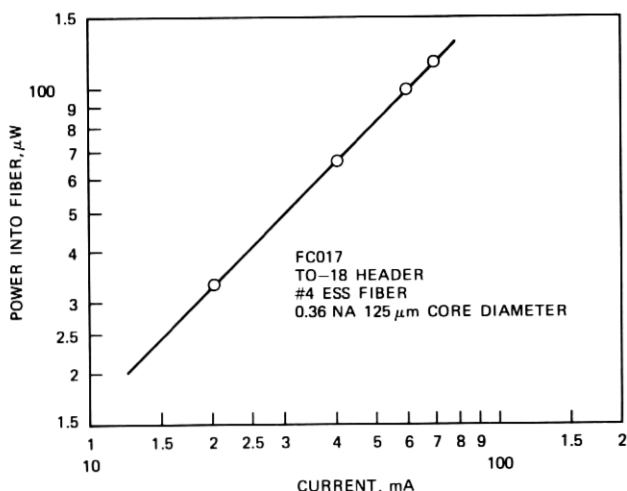

Fig. 2—Typical optical power of restricted contact area planar, single heterojunction, optical-link LED butt-coupled into a 0.36-NA, 125-μm core diameter, step-index fiber.
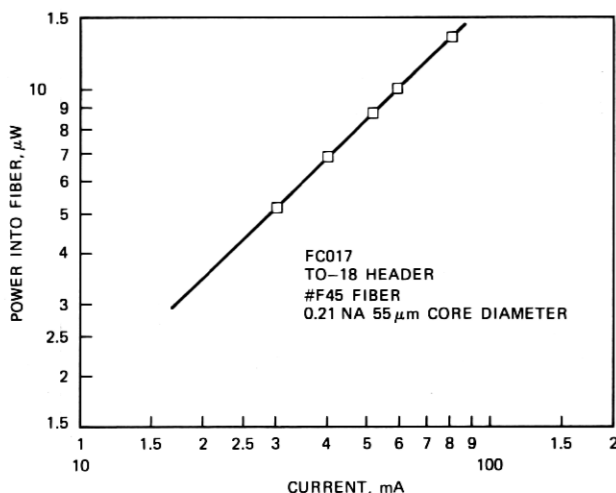
Fig. 3—Typical optical power of restricted contact area planar, single heterojunction, optical-link LED butt-coupled into 0.23-NA, 55-μm core diameter, graded-index fiber.

coupled power by no more than 15 percent. This relatively small reduction is tolerable in view of the resulting simplicity of processing and very high planar device fabrication yield.

V. RELIABILITY

Accelerated aging tests at elevated temperatures and under forward bias are being performed on broad area and restricted contact area devices to determine long-term stability. The LED chips are mounted on TO-18 headers without encapsulation. They are being aged at the anticipated operating current in the optical link system, which is 60 mA forward current pulsed at 10 MHz with a 50-percent duty cycle. The power dissipated under these conditions gives a 10°C rise in junction temperature (T_j) over the ambient temperature (T_a).

Ten randomly chosen diodes were aged at each of three ambient temperatures (100, 150, and 200°C) with each group of 10 containing diodes taken from three different epitaxial runs. Growth parameters during the three runs were the same. Figure 4 shows the logarithm of the average of the degradation in quantum efficiency (η/η_0) for each group of diodes versus $t^{1/2}$. At each temperature, an initial degradation of about 5 percent in the first few hours is followed by a slower degradation process. At each temperature, the data for the slow process fall along a straight line on this plot, suggesting that the process may be described phenomenologically by

$$\frac{\eta}{\eta_0} = \exp\left[-\left(\frac{t}{\tau_{1/2}}\right)^{1/2}\right], \tag{1}$$

where $\tau_{1/2}$ is the time constant for the process and is found from the slope of the line.

A quantity of interest in predicting failure rates is the mean time to failure (MTTF), where failure for a single device is defined as $\eta/\eta_0 = 50$ percent. Only the diodes being aged at $T_a = 200°C$ have degraded enough so that the data may be extrapolated to $\eta/\eta_0 = 50$ percent with confidence. However, ignoring the initial fast component of degradation, $\tau_{1/2}$ is equal to 2.08 times the MTTF. Therefore, values of $\tau_{1/2}$ calculated from the slopes of the lines have been used to estimate MTTF at each temperature. For $T_a = 100, 150,$ and $200°C$ (or $T_j = 114, 164, 214°C$), the values of MTTF found in this way are 1.3×10^6, $1.7 \times$
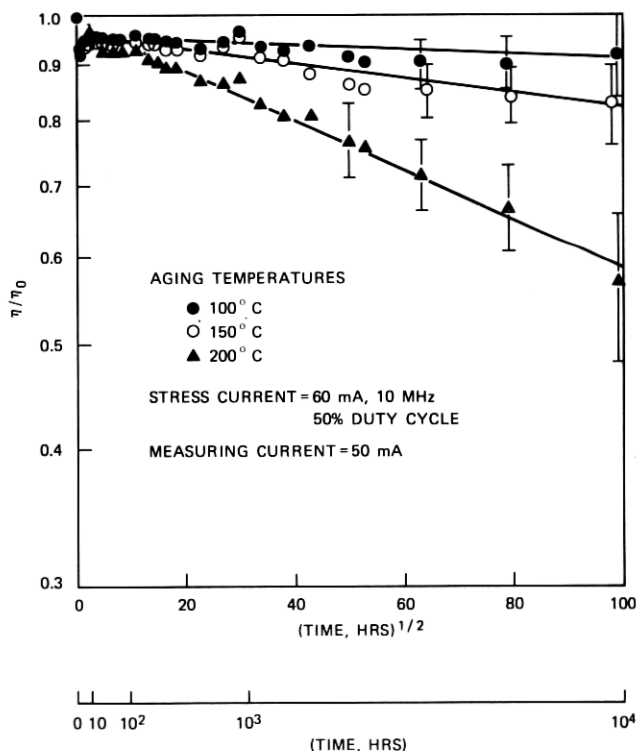

Fig. 4—Reliability performance of restricted contact area planar, single heterojunction optical-link LED. Results of long-term aging under 60-mA, 10-MHz, 50-percent duty cycle at various temperatures. The log of relative degraded efficiency averaged for 10 diodes ($\log \bar{\eta}/\bar{\eta}_0$) is plotted vs the square root of time.

10^5, and 1.6×10^4 hours, respectively. These times yield an activation energy for the process of 0.75 eV.[15] At the operating temperatures expected in an optical link ($T_a = 60°C$ or $T_j = 74°C$), the MTTF is 2.2×10^7 hours. The devices fail with a lognormal distribution with $\sigma = 0.4$.[15] Using lognormal statistics,[16] we estimate that, for continuous operation at 60 mA forward current pulsed at 10 MHz with a 50 percent duty cycle, the failure rates for service lives of 10, 20, or 40 years will be less than 1 FIT.

VI. SUMMARY

We have discussed simple geometry, planar, single heterojunction LEDs. The salient features of these LEDs are (i) simplicity—the single heterojunction and diode geometry makes large scale reproducibility more easily attainable; (ii) exceptional stability—even when operated at higher effective current densities (up to 700 A/cm^2) the confined contact structures have proven highly reliable with predicted failure rates of 1 FIT for a 40-year service life; (iii) adequate optical power— an excess of 100 μW of optical power can be launched into a 0.36-NA 125-μm core diameter, step-index fiber and an excess of 10 μW into a 0.23-NA, 55-μm core diameter, graded-index fiber, (iv) fast response times—electroluminescence rise and fall times are $\approx$3 ns each, making these LEDs adequate for data transmission rates as high as 100 Mb/s. These devices have been used as sources in prototype subsystems under development for use in electronic switching systems.

VII. ACKNOWLEDGMENTS

REFERENCES

1. L. R. Dawson, V. G. Keramidas, and C. L. Zipfel, B.S.T.J., *59*, No. 2 (February 1980), p. 161.
2. W. G. French, J. B. MacChesney, P. B. O'Connor, G. W. Tosker, B.S.T.J., *53*, No. 5 (May–June 1974), p. 951.

3. W. H. Hackett, Jr., C. A. Bracket, L. E. Howarth, R. G. Smith, A. W. Warner, M. DiDomenico, Jr., R. S. Riggs, Topical Meeting on Optical Fiber Transmission II, Williamsburg, Va., February 22–24, 1977.
4. C. A. Burrus, and B. I. Miller, Opt. Commun. *4* (1971), p. 307.
5. L. R. Dawson, J. Appl. Phys., *48* (1977), p. 2485.
6. V. G. Keramidas, "GaAs and Related Compounds," Inst. Phys. Conf. Series No. 45 (1978), p. 396.
7. C. A. Burrus, and E. A. Ulmer, Proc. IEEE (1979), p. 1263.
8. R. W. Dawson, C. A. Burrus, Appl. Opt., *10* (1971), p. 2367.
9. J. C. Dyment, J. C. North, and L. A. D'Asaro, J. Appl. Phys., *44* (1973), p. 207.
10. A. G. Foylt et al., Solid State Elec., *12* (1969), p. 209.
11. J. Heinen, W. Huber, and W. Harth, Electron. Lett., *12* (1976), p. 553.
12. R. C. Goodfellow and A. W. Mabbitt, Electron. Lett., *12* (1976), p. 50.
13. A. K. Chin, G. W. Berkstresser, and V. G. Keramidas, B.S.T.J., *58*, No. 7 (September 1979), p. 1579.
14. M. Ettenberg, H. Kressel, and S. L. Gilbert, J. Appl. Phys., *44* (1973), p. 827.
15. C. L. Zipfel, V. G. Keramidas, and R. H. Saul, 1979 Device Research Conference, Boulder, Colo., June 1979.
16. A. S. Jordan, Microelectronics and Reliability, *18*, No. 3 (1978), p. 267.